Swarming morlet wavelet

by Irwan Fathurrochman

Submission date: 02-Oct-2022 08:53AM (UTC+0700)
Submission ID: 1913990075
File name: Irwan_1-s2.0-S2352914822002179-main.pdf (744.45K)
Word count: 5191
Character count: 33591

Swarming morlet wavelet neural network procedures for the mathematical robot system

Peerapongpat Singkibud, Zulqurnain Sabir, Irwan Fathurrochman, Sharifah E. Alhazmi, Mohamed Ali

PII: S2352-9148(22)00217-9

DOI: https://doi.org/10.1016/j.imu.2022.101081

Reference: IMU 101081

To appear in: *Informatics in Medicine Unlocked*

Received Date: 20 August 2022

Revised Date: 4 September 2022

Accepted Date: 5 September 2022

Please cite this article as: Singkibud P, Sabir Z, Fathurrochman I, Alhazmi SE, Ali M, Swarming morlet wavelet neural network procedures for the mathematical robot system, *Informatics in Medicine Unlocked* (2022), doi: https://doi.org/10.1016/j.imu.2022.101081.

Swarming Morlet wavelet neural network procedures for the mathematical robot system

Peerapongpat Singkibud[a], Zulqurnain Sabir[b,c], Irwan Fathurrochman[d], Sharifah E Alhazmi[e], Mohamed R. Ali[f]

[a]Department of Applied Mathematics and Statistics, Faculty of Sciences and Liberal Arts, Rajamangala University of Technology Isan, Nakhon Ratchasima 30000, Thailand.
[b]Department of Mathematics and Statistics, Hazara University, Mansehra, Pakistan
[c]Department of Mathematical Sciences, UAE University, P. O. Box 15551, Al Ain, UAE
[d]Department of Islamic Educational Management, Institute Agama Islam Negeri Curup, Rejang Lebong, Indonesia
[e]Mathematics Department, Al-Qunfudah University College, Umm Al-Qura University, Mecca, KSA
[f] Faculty of Engineering and Technology, Benha University, Cairo, Egypt

Abstract: The task of this work is to present the solutions of the mathematical robot system (MRS) to examine the positive coronavirus cases through the artificial intelligence (AI) based Morlet wavelet neural network (MWNN). The MRS is divided into two classes, infected $I(\theta)$ and Robots $R(\theta)$. The design of the fitness function is presented by using the differential MRS and then optimized by the hybrid of the global swarming computational particle swarm optimization (PSO) and local active set procedure (ASP). For the exactness of the AI based MWNN-PSOIPS, the comparison of the results is presented by using the proposed and reference solutions. The reliability of the MWNN-PSOASP is authenticated by extending the data into 20 trials to check the performance of the scheme by using the statistical operators with 10 hidden numbers of neurons to solve the MRS.

Keywords*:* mathematical Robot system; Artificial intelligence; Particle swarm optimization; Active set procedure; Morlet wavelet; Numerical solutions.

Swarming Morlet wavelet neural network procedures for the mathematical robot system

Peerapongpat Singkibud[a], Zulqurnain Sabir[b,c], Irwan Fathurrochman[d], Sharifah E Alhazmi[e], Mohamed R. Ali[f]

[a]Department of Applied Mathematics and Statistics, Faculty of Sciences and Liberal Arts, Rajamangala University of Technology Isan, Nakhon Ratchasima 30000, Thailand.
[b]Department of Mathematics and Statistics, Hazara University, Mansehra, Pakistan
[c]Department of Mathematical Sciences, UAE University, P. O. Box 15551, Al Ain, UAE
[d]Department of Islamic Educational Management, Institute Agama Islam Negeri Curup, Rejang Lebong, Indonesia
[e]Mathematics Department, Al-Qunfudah University College, Umm Al-Qura University, Mecca, KSA
[f] Faculty of Engineering and Technology, Benha University, Cairo, Egypt

Abstract: The task of this work is to present the solutions of the mathematical robot system (MRS) to examine the positive coronavirus cases through the artificial intelligence (AI) based Morlet wavelet neural network (MWNN). The MRS is divided into two classes, infected $I(\theta)$ and Robots $R(\theta)$. The design of the fitness function is presented by using the differential MRS and then optimized by the hybrid of the global swarming computational particle swarm optimization (PSO) and local active set procedure (ASP). For the exactness of the AI based MWNN-PSOIPS, the comparison of the results is presented by using the proposed and reference solutions. The reliability of the MWNN-PSOASP is authenticated by extending the data into 20 trials to check the performance of the scheme by using the statistical operators with 10 hidden numbers of neurons to solve the MRS.

Keywords*:* mathematical Robot system; Artificial intelligence; Particle swarm optimization; Active set procedure; Morlet wavelet; Numerical solutions.

1. Introduction

The prevalence of communicable diseases has long been a problem over the world. To name only few viruses, dengue fever (DF), which affects 2.5 billion people worldwide, is the most dangerous, contagious, and pandemic diseases. Due to ignorance and insufficient knowledge, DF is generally observed in the warmest areas in the world, such as South Asia [1-2]. There are deadly, contagious illnesses on every region of the planet, including HIV. HIV spreads like some of the other infections, and during the past few decades, numerous civilian casualties have been observed [3-5]. Lassa disease is a very severe illness that is primarily found in underdeveloped areas [6]. Malaria is another prevalent condition that transmits through indirect contact between

hosts [7-8]. According to world health organization statistics, there have been claimed to have been one million cases from malaria, which primarily affects pregnant women and children from the United States and South Africa [9]. An additional contagious, fatal virus called Ebola is spread by people to infected animals [10]. The world has just been plagued by a deadly coronavirus epidemic that has had a negative impact on global economies, education sectors, sport events, tourism, business and airline sectors [11-13]. One human can infect another with the coronavirus [14]. Since the beginning of the coronavirus, it has abruptly halted people from living busy, rapid lives and has caused uncertainty throughout the entire planet. More deadly than before, it has now appeared in a wide variety of shapes, variants, and phases. It had an influence on the economies of numerous developed and emerging nations. Currently, one, two or three doses of various vaccines have been used throughout the world to begin the immunization process [15].

The majority of infections lack effective treatments or vaccines. Consequently, only a few medical safeguards have been approved to prevent the propagation of these infections. Because of this, the globe adopted several other precautions to prevent the spread of such infections, such as quarantines, social distances, handwashing, avoiding crowded areas, etc. One of the main causes of disease is free healthcare, which is provided by medical personnel such as doctors and nurses. A serious issue for the entire world is being caused by the rising number of positive coronavirus cases [16-17]. Numerous analytical/numerical approaches to the problem of infectious illnesses have been developed. To mention some of them are Mickens employed a vaccination strategy based on distinct time to prevent the transmission of recurring viruses. Newton's embedded approach using the optimal control is applied by Ogren et al. [18] for the SIR dynamical system. The spatial measles outbreak was used on the fractional SIR epidemic by Goufo et al. [19]. Another few research projects based on infectious systems and theoretical advancements are given in these references [20–23]. Consequently, using robots to identify coronavirus-positive patients is crucial. The benefit of using robots is that they can provide medical assistance for those who are ill and stop the coronavirus spread. The dynamics of the MRS is divided into two classes, infected $I(\theta)$ and Robots $R(\theta)$, mathematically presented as [24]:

$$\begin{cases} I'(\theta) = \left(a - bR(\theta) - u\right) I(\theta) + C(I), & I_0 = i_1, \\ R'(\theta) = c - dR(\theta), & R_0 = i_2, \end{cases} \tag{1}$$

where $I(\theta)$ and $R(\theta)$ indicate the infected and Robot populations. a and c represent the newly infected individual and robot production rates. $C(I)$ is the migration factor using the human infected population, u shows the infected individual rate to death due to coronavirus, b is the detection rate based infected robots individual, d provides the stopping robot functioning rate, θ is the time, while i_1 and i_2 are the initial conditions (ICs).

The purpose of this study is to present the solutions of the mathematical robot system (MRS) to examine the positive coronavirus cases through the artificial intelligence (AI) based Morlet wavelet neural network (MWNN) under the optimization of the hybrid global swarming computational particle swarm optimization (PSO) and local active set procedure (ASP). The AI based stochastic solvers have been used in many applications, some of them are singular models [25-26], periodic differential models [27], food chain models [28-30] and economic/environmental models [31]. These presented stochastic based applications motivated the authors to explore the AI based MWNN-PSOIPS for solving the nonlinear MRS to achieve the stable and reliable numerical performances. Few of the novel features related to MWNN-PSOIPS are presented as:

- The solutions of the nonlinear MRS to examine the positive coronavirus cases using the AI based stochastic computing PSOIPS are presented.
- The stochastic AI based MWNN-PSOIPS is efficiently implemented to present the solutions of the nonlinear MRS.
- The exactness of the AI based MWNN-PSOIPS is obtained through the comparison of the proposed and reference results.
- The corroboration of AI based MWNN-PSOIPS is obtained using the statistical Theil inequality coefficient (TIC) and mean square error (MSE) to validate the dependability of the nonlinear MRS to examine the positive coronavirus cases.
- The absolute error (AE) is performed in good measures, which authenticates the accuracy of the MWNN-PSOIPS.

The remaining structure of the paper is presented as: Sect 2 presents the structure of the MWNN-PSOIPS. Sect 3 provides the comprehensive performances of the solutions. Sect 5 provides the conclusions along with upcoming reports.

2. Methodology

The current section presents the AI based MWNN-PSOIPS formulation to solve the MRS. Fig.1 shows the graphical performances of the AI based MWNN-PSOIPS.

2.1 MWNN-PSOIPS design

The AI based MWNN-PSOIPS structure is presented to solve the MRS, which is shown in Eq. (1). The proposed solutions are represented as $\hat{I}$ and $\hat{R}$ with the derivatives of 1st kind is shown as:

$$\left[\hat{I}(\theta),\hat{R}(\theta)\right]=\left[\sum_{q=1}^{s} y_{I,q}N(\Psi_{I,q}\theta+z_{I,q}),\ \sum_{q=1}^{s} y_{R,q}N(\Psi_{R,q}\theta+z_{R,q})\right],$$
$$\left[\hat{I}'(\theta),\hat{R}'(\theta)\right]=\left[\sum_{q=1}^{s} y_{I,q}N'(\Psi_{I,q}\theta+z_{I,q}),\ \sum_{q=1}^{s} y_{R,q}N'(\Psi_{R,q}\theta+z_{R,q})\right], \quad (2)$$

where s presents the neurons and the unknown vectors $[\boldsymbol{y},\boldsymbol{\Psi},\boldsymbol{z}]$ are given as:

$\boldsymbol{W}=[\boldsymbol{W}_I,\boldsymbol{W}_R]$, for $\boldsymbol{W}_R=[\boldsymbol{y}_R,\boldsymbol{\Psi}_R,\boldsymbol{z}_R]$ and $\boldsymbol{W}_I=[\boldsymbol{y}_I,\boldsymbol{\Psi}_I,\boldsymbol{z}_I]$, where

$\boldsymbol{y}_I=[y_{I,1},y_{I,2},...,y_{I,s}]$, $\boldsymbol{y}_R=[y_{R,1},y_{R,2},...,y_{R,s}]$, $\boldsymbol{\Psi}_I=[\Psi_{I,1},\Psi_{I,2},...,\Psi_{I,s}]$,

$\boldsymbol{\Psi}_R=[\Psi_{R,1},\Psi_{R,2},...,\Psi_{R,s}]$, $\boldsymbol{z}_I=[z_{I,1},z_{I,2},...,z_{I,s}]$, $\boldsymbol{z}_R=[z_{R,1},z_{R,2},...,z_{R,s}]$.

The AI based MWNN have been applied first time to solve the MRS. The Morlet function is mathematically depicted as:

$$N(\theta)=\cos(1.75\theta)\exp(-\frac{1}{2}\theta^2). \quad (3)$$

Eq. (2) is updated as:

$$\left[\hat{I}(\theta),\hat{R}(\theta)\right]=\begin{bmatrix}\sum_{q=1}^{s} y_{I,q}\cos\left(1.75(\Psi_{I,q}\theta+z_{Iq})\right)e^{-0.5(\Psi_{Iq}\theta+z_{Iq})^2},\\ \sum_{q=1}^{s} y_{R,q}\cos\left(1.75(\Psi_{R,q}\theta+z_{Rq})\right)e^{-0.5(\Psi_{Rq}\theta+z_{Rq})^2}\end{bmatrix},$$

$$\left[\hat{I}'(\theta),\hat{R}'(\theta)\right]=\left[\sum_{q=1}^{s}2y_{Iq}\Psi_{Iq}\left(\frac{e^{(\Psi_{Iq}\theta+z_{Iq})}}{1+\left(e^{(\Psi_{Iq}\theta+z_{Iq})}\right)^2}\right),\sum_{q=1}^{s}2y_{Rq}\Psi_{Rq}\left(\frac{e^{(\Psi_{Rq}\theta+z_{Rq})}}{1+\left(e^{(\Psi_{Rq}\theta+z_{Rq})}\right)^2}\right)\right], \quad \textbf{(4)}$$

To present the solution of the MRS, a merit function is presented as:

$$M_F=M_{F-1}+M_{F-2}+M_{F-3}, \quad \textbf{(5)}$$

where, M_{F-1} and M_{F-2} are the merit functions using the infected and Robot population, $I(\theta)$ and $R(\theta)$ that are constructed using the different MRS, while the construction of M_{F-3} is based on the ICs of the MRS, shown as:

$$M_{F-1}=\frac{1}{N}\sum_{q=1}^{K}\left(\hat{I}'_q-(a-b\hat{R}_q-u)\hat{I}_q-C(\hat{I}_q)\right)^2, \quad \textbf{(6)}$$

$$M_{F-2}=\frac{1}{N}\sum_{q=1}^{K}\left(\hat{R}'_q+d\hat{R}_q-c\right)^2, \quad \textbf{(7)}$$

$$M_{F-3}=\frac{1}{2}\left(\left(\hat{I}_0-i_1\right)^2+\left(\hat{R}_0-i_2\right)^2\right), \quad \textbf{(8)}$$

$Kh=1,\ \hat{I}_q=\hat{I}\left(\theta_q\right),\ \hat{R}_q=\hat{R}\left(\theta_q\right),\ \theta_q=qh.$

2.2 Optimization: PSOASP

The current section shows the procedure of optimization using the PSOASP to solve the MRS. Fig. 1 shows the workflow illustrations based on the MWNN-PSOASP for the MRS.

The method for computationally optimizing global search swarming approach called PSO is used to substitute the genetic algorithms. The PSO technique was first established during the last decade by Kennedy and Eberhart [32]. PSO displays the outcomes of multiple intricate systems that manage a specific population utilizing the technique of optimum training. PSO can be completed easily due to the minimal storage capacity [33]. In recent decades, PSO is used in various submissions, e.g., engineering systems [34], multi-objective multimodal methods [35],

solar energy models [36], cataloguing the photovoltaic based single/double/triple parameter diode [37], plant diseases [38], image organization [39], particle filter noise reduction based on the analysis of mechanical accountability [30] and green coal production networks [41]. These submissions stimulated the authors to perform the swarming approaches for the MRS.

A local search optimization technique known as active set programming is used to improve the performance of unconstrained and convex models. Recently, ASP is applied in various applications, some of them are realizable safety critical control [42], linearly non-lipschitz constrained nonconvex optimization [43], lung tumor detection and classification [44], atrial fibrillation detection based on transfer learning [45], characterizations of discrete-time descriptor systems [46], pressure-dependent models of water distribution systems [47] and embedded model predictive control [48]. The AI based MWNN-PSOASP is implemented to present the numerical solutions of the MRS. Fig. 1 shows the workflow illustration of MWNN-PSOASP for the MRS

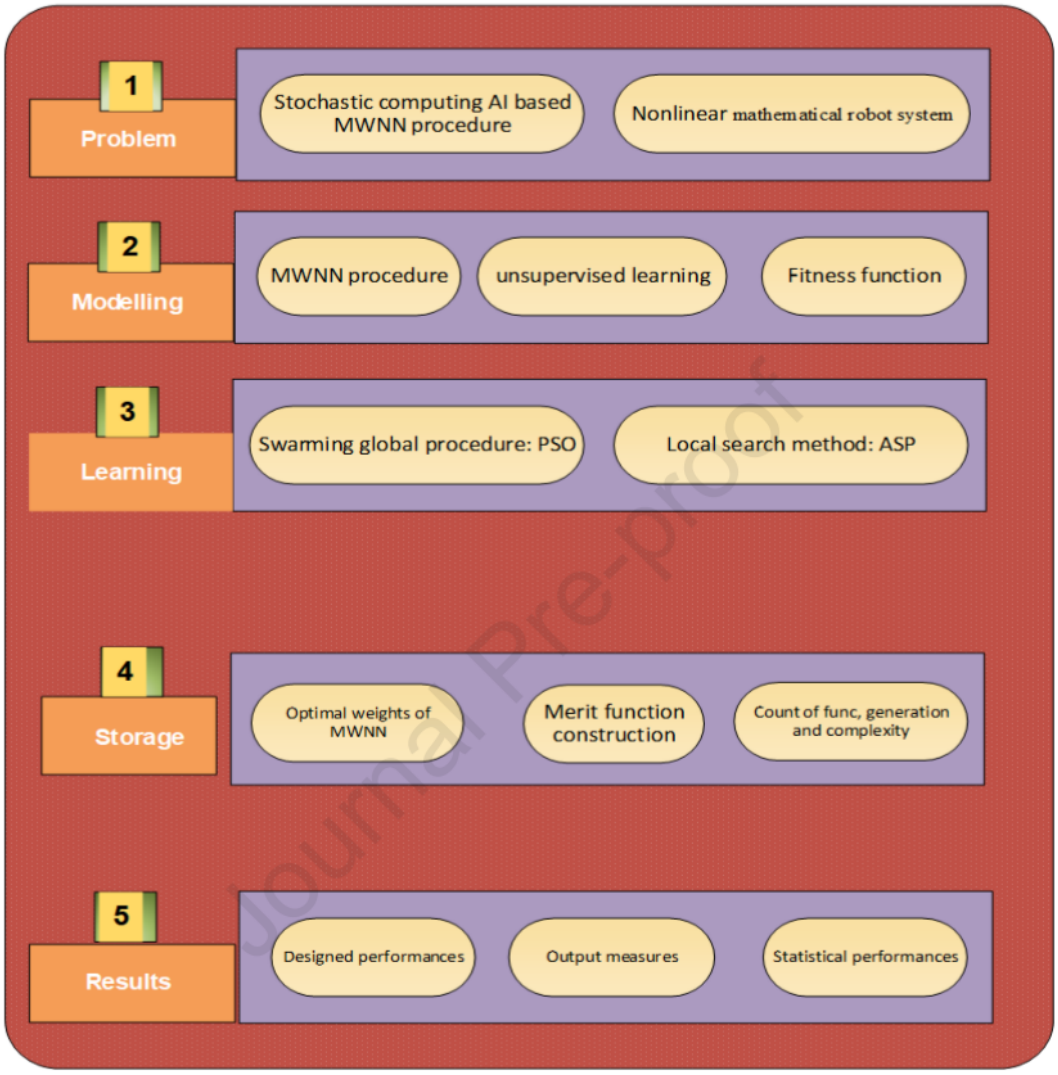

Figure 1. Workflow illustration of MWNN-PSOASP for the MRS

The pseudocode of the current study based on the optimization procedure to solve the MRS is presented below as:

Pseudocode using the MWNN-PSOASP for the MRS

PSO starts

Inputs: The values of the chromosomes $\boldsymbol{W} = [\boldsymbol{W}_I, \boldsymbol{W}_R]$, for $\boldsymbol{W}_R = [\boldsymbol{y}_R, \boldsymbol{\Psi}_R, \boldsymbol{z}_R]$ and $\boldsymbol{W}_I = [\boldsymbol{y}_I, \boldsymbol{\Psi}_I, \boldsymbol{z}_I]$.

Population: The chromosomes for the q^{th} variables are

$\boldsymbol{y}_I=[y_{I,1},y_{I,2},...,y_{I,s}]$, $\boldsymbol{y}_R=[y_{R,1},y_{R,2},...,y_{R,s}]$, $\boldsymbol{\Psi}_I=[\Psi_{I,1},\Psi_{I,2},...,\Psi_{I,s}]$,
$\boldsymbol{\Psi}_R=[\Psi_{R,1},\Psi_{R,2},...,\Psi_{R,s}]$, $\boldsymbol{z}_I=[z_{I,1},z_{I,2},...,z_{I,s}]$, $\boldsymbol{z}_R=[z_{R,1},z_{R,2},...,z_{R,s}]$.

Output: The optimal swarming measures are $\boldsymbol{W}_{\mathbf{B.PSO}}$

Initialization: Construct the weight matrix ($\boldsymbol{W}$) for the performances of the real bounds to elect the chromosome. $\boldsymbol{W}$ shows the initial population. Indicate the primary random swarm to set the PSO and 'gaoptimset'.

Fitness Evaluation: Obtain the M_F by using the Eqs (5) to (8).

Stopping criteria: Terminate if TolFun =10^{-19}, population span = (-15,15), Initial weights= decreasing, particlesize = 55, HybridFcn =@fmincon, SwarmSize=100, velocity span = (-3,3), then Go to [**storage**].

Ranking: Present the Rank "$\boldsymbol{W}$" using the "$\boldsymbol{P}$" based on the M_F.

Storage: $\boldsymbol{W}_{\mathbf{B.PSO}}$ presents the optimal weights, M_F, complexity, generations and count of function using the execution of PSO.

Swarming optimization procedure Ends

ASP starts

Inputs: $\boldsymbol{W}_{\mathbf{B.\ PSO}}$

Output: The Optimal measures using PSOASP are $\boldsymbol{W}_{\boldsymbol{PSOASP}}$

Initialize: Regulate the generations, constrains and other performances.

Dismiss: ASP stops, when the values of the generations are 740, M_F = 10^{-20}, MaxFunEvals = 275000, and TolFun/Con/X=10^{-19} obtained.

Fitness: M_F for each $\boldsymbol{W}$ based population $\boldsymbol{P}$ for (5) to (8).

Modifications: Fmincon of the ASP for the fine-tune of $\boldsymbol{W}$.

Accumulate: M_F, $\boldsymbol{W}_{\mathbf{B.\ PSO}}$, epochs, time, and count of function.

ASP ends

2.3. Statistical performances

The current section shows the mathematical performances based on the TIC and MSE for solving the MRS, which is shown as:

$$[\mathrm{TIC}_I,\mathrm{TIC}_R]=\left(\frac{\sqrt{\frac{1}{n}\sum_{q=1}^{n}\left(I_q-\hat{I}_q\right)^2}}{\left(\sqrt{\frac{1}{n}\sum_{q=1}^{n}I_q^2}+\sqrt{\frac{1}{n}\sum_{q=1}^{n}\hat{I}_q^2}\right)},\frac{\sqrt{\frac{1}{n}\sum_{q=1}^{n}\left(R_q-\hat{R}_q\right)^2}}{\left(\sqrt{\frac{1}{n}\sum_{q=1}^{n}R_q^2}+\sqrt{\frac{1}{n}\sum_{q=1}^{n}\hat{R}_q^2}\right)}\right), \tag{9}$$

$$[\mathrm{MSE}_I,\mathrm{MSE}_R]=\left[\sum_{q=1}^{n}\left(I_q-\hat{I}_q\right)^2,\ \sum_{q=1}^{n}\left(R_q-\hat{R}_q\right)^2\right]. \tag{10}$$

3. Simulation and results

This section indicated the numerical simulations based on the AI based MWNN-PSOASP for the MRS. The comparison performances based on the reference and obtained results are presented to authenticate the consistency of the procedure. Consider $d=0.2$, $c=0.1$, $C(I)=C=2$, $b=0.1$, $a=0.5$, $u=0.3$, $i_1=0.6$ and $i_2=0.5$ are presented as:

$$\begin{cases} I'(\theta)=\left(0.5-0.1R(\theta)-0.3\right)I(\theta)+2, & I_0=0.5, \\ R'(\theta)=0.1-0.2R(\theta), & R_0=0.6. \end{cases} \tag{11}$$

A M_F takes the form as:

$$\begin{aligned} M_F=&\frac{1}{N}\sum_{q=1}^{K}\left(\left(\hat{I}'_q-0.5\hat{I}_q+0.1\hat{R}_q\hat{I}_q+0.3\hat{I}_q+2\right)^2+\left(\hat{R}'_q-0.1+0.2\hat{R}_q\right)^2\right) \\ &+\frac{1}{2}\left(\left(\hat{I}_0-0.5\right)^2+\left(\hat{R}_0-0.6\right)^2\right) \end{aligned} \tag{12}$$

The optimization performances using the AI based MWNN-PSOASP for the MRS are provided for twenty independent trials to perform the parameter of the model. The values of the numerical outputs have been achieved in the [0, 1] with the step size 0.05. The proposed values of the $I(\theta)$ and $R(\theta)$ are shown as:

$$\begin{aligned} \hat{I}(\theta)=&3.41\cos\left(\frac{4}{3}(0.61\theta-2.48)\right)e^{-\frac{1}{2}(0.61\theta-2.48)^2}+0.56\cos\left(\frac{4}{3}(1.58\theta+0.97)\right)e^{-\frac{1}{2}(1.58\theta+0.97)^2} \\ &-0.57\cos\left(\frac{4}{3}(1.42\theta+2.34)\right)e^{-\frac{1}{2}(1.42\theta+2.34)^2}+1.16\cos\left(\frac{4}{3}(0.61\theta+0.68)\right)e^{-\frac{1}{2}(0.61\theta+0.68)^2} \\ &+2.24\cos\left(\frac{4}{3}(1.12\theta+2.75)\right)e^{-\frac{1}{2}(1.12\theta+2.75)^2}-0.31\cos\left(\frac{4}{3}(0.98\theta+1.89)\right)e^{-\frac{1}{2}(0.98\theta+1.89)^2} \\ &-1.29\cos\left(\frac{4}{3}(1.48\theta+1.34)\right)e^{-\frac{1}{2}(1.48\theta+1.34)^2}-2.83\cos\left(\frac{4}{3}(-0.1\theta+0.25)\right)e^{-\frac{1}{2}(-0.1\theta+0.25)^2} \\ &-2.27\cos\left(\frac{4}{3}(-0.4\theta+0.71)\right)e^{-\frac{1}{2}(-0.4\theta+0.71)^2}+3.61\cos\left(\frac{4}{3}(2.50\theta+4.80)\right)e^{-\frac{1}{2}(2.50\theta+4.80)^2}, \end{aligned} \tag{13}$$

$$\hat{R}(\theta) = -0.1\cos\left(\frac{4}{3}(0.18\theta+0.55)\right)e^{-\frac{1}{2}(0.18\theta+0.55)^2} + 0.26\cos\left(\frac{4}{3}(0.18\theta+1.24)\right)e^{-\frac{1}{2}(0.18\theta+1.24)^2}$$
$$+0.14\cos\left(\frac{4}{3}(-0.08\theta-0.5)\right)e^{-\frac{1}{2}(-0.08\theta-0.5)^2} + 0.61\cos\left(\frac{4}{3}(0.20\theta+2.01)\right)e^{-\frac{1}{2}(0.20\theta+2.01)^2}$$
$$+0.05\cos\left(\frac{4}{3}(-0.2\theta+0.09)\right)e^{-\frac{1}{2}(-0.2\theta+0.09)^2} + 0.03\cos\left(\frac{4}{3}(-0.7\theta-1.70)\right)e^{-\frac{1}{2}(-0.7\theta-1.70)^2} \quad \textbf{(14)}$$
$$-0.008\cos\left(\frac{4}{3}(0.3\theta+0.030)\right)e^{-\frac{1}{2}(0.3\theta+0.03)^2} + 0.34\cos\left(\frac{4}{3}(-0.1\theta-0.78)\right)e^{-\frac{1}{2}(-0.1\theta-0.78)^2}$$
$$+0.2\cos\left(\frac{4}{3}(0.02\theta-0.098)\right)e^{-\frac{1}{2}(0.02\theta-0.09)^2} - 0.15\cos\left(\frac{4}{3}(-0.1\theta+0.06)\right)e^{-\frac{1}{2}(-0.1\theta+0.06)^2},$$

Tables 3 and 4 indicates the statistical performances of the $I(\theta)$ and $R(\theta)$ for the MRS. The Mean, Maximum (Max), standard deviation (STD), Median (MD), Minimum (Min), and Semi-interquartile range (SIR) for the MRS are presented in Table 1 and Table 2. The mathematical performance of the SIR is the difference of ½ times of quartile 3rd and 1st. The Mean, STD, MD and SIR performances have been performed for both $I(\theta)$ and $R(\theta)$ of the MRS are 10^{-06} to 10^{-07}. The Max values shows the poor results but found as 10^{-05} to 10^{-06} for both $I(\theta)$ and $R(\theta)$. The Min performances shows the good results, which are found for both classes are 10^{-07} to 10^{-11}. These calculated operator small measures represent the dependability of the AI based on the MWNN-PSOASP for the MRS.

Table 1: Statistical operator performances for $I(\theta)$

θ	$I(\alpha)$					
	Mean	**Max**	**STD**	**MD**	**Min**	**SIR**
0	4.54674E-07	4.90402E-06	1.07541E-06	1.75826E-07	7.10649E-11	2.39063E-07
0.05	8.50202E-07	6.91587E-06	1.50625E-06	4.09634E-07	5.03369E-09	2.34732E-07
0.1	1.43577E-06	6.75494E-06	1.59467E-06	9.45636E-07	9.66264E-08	6.37282E-07
0.15	2.50968E-06	1.03194E-05	2.36168E-06	1.92842E-06	1.04942E-07	1.25302E-06
0.2	3.21751E-06	1.37793E-05	3.14077E-06	2.85585E-06	1.52113E-07	2.02217E-06
0.25	3.31684E-06	1.42339E-05	3.39703E-06	2.66063E-06	1.81681E-08	2.22107E-06
0.3	2.85017E-06	1.21896E-05	3.13704E-06	2.27382E-06	5.16728E-08	1.86375E-06
0.35	2.15496E-06	9.03015E-06	2.47878E-06	1.52121E-06	1.43166E-08	9.39160E-07
0.4	1.31191E-06	7.96198E-06	1.90939E-06	6.86554E-07	1.83868E-08	3.92892E-07
0.45	1.03345E-06	5.92670E-06	1.41285E-06	4.92309E-07	4.13522E-08	5.37661E-07
0.5	1.24158E-06	4.48179E-06	1.12813E-06	8.96362E-07	4.58559E-08	6.35915E-07

0.55	1.19577E-06	6.83674E-06	1.41559E-06	8.39599E-07	2.50308E-07	4.55329E-07
0.6	1.17749E-06	9.10337E-06	1.95084E-06	7.05512E-07	8.88368E-09	5.74924E-07
0.65	1.91972E-06	1.08727E-05	2.35191E-06	1.36164E-06	5.64084E-08	7.46043E-07
0.7	2.77014E-06	1.17677E-05	2.78416E-06	2.18574E-06	1.41055E-07	1.38304E-06
0.75	3.40234E-06	1.15413E-05	3.05703E-06	2.72830E-06	3.46908E-08	2.05816E-06
0.8	3.48297E-06	1.08901E-05	3.06579E-06	2.72537E-06	3.80029E-07	2.16012E-06
0.85	3.02570E-06	1.06894E-05	2.65767E-06	2.49113E-06	3.94092E-07	1.68071E-06
0.9	2.14565E-06	9.15875E-06	2.30348E-06	1.42499E-06	8.90565E-08	8.20232E-07
0.95	1.61955E-06	7.63815E-06	2.31111E-06	6.39825E-07	1.01675E-07	4.31817E-07
1	1.60816E-06	7.03658E-06	2.24844E-06	6.89440E-07	3.11178E-08	6.28636E-07

Table 2: Statistical operator performances for $R(\theta)$

θ	$R(\theta)$					
	Mean	**Max**	**STD**	**MD**	**Min**	**SIR**
0	6.99460E-07	4.08335E-06	1.18329E-06	1.28407E-07	4.52558E-11	4.59012E-07
0.05	1.02726E-06	4.77161E-06	1.19940E-06	6.79014E-07	6.14489E-08	4.07815E-07
0.1	1.10895E-06	4.73802E-06	1.41447E-06	4.51034E-07	2.76715E-08	7.40714E-07
0.15	1.43775E-06	5.26152E-06	1.58219E-06	5.56007E-07	1.35583E-07	1.31568E-06
0.2	1.69645E-06	5.42398E-06	1.62995E-06	1.06686E-06	5.07068E-08	1.32827E-06
0.25	1.77104E-06	6.39889E-06	1.64773E-06	1.51742E-06	3.35034E-08	8.96608E-07
0.3	1.65634E-06	6.34479E-06	1.67096E-06	1.48981E-06	1.95450E-08	7.47756E-07
0.35	1.58544E-06	5.54289E-06	1.41214E-06	9.79522E-07	2.67251E-07	8.58269E-07
0.4	1.37958E-06	4.31668E-06	1.08515E-06	9.64483E-07	2.94522E-07	7.07770E-07
0.45	1.09051E-06	2.93435E-06	8.50722E-07	9.42918E-07	6.43934E-08	5.79809E-07
0.5	9.11132E-07	2.70075E-06	8.70778E-07	5.39011E-07	4.37776E-08	7.04615E-07
0.55	1.01544E-06	3.27748E-06	1.07882E-06	5.01748E-07	5.62508E-09	8.23989E-07
0.6	1.37673E-06	4.22142E-06	1.17568E-06	1.05988E-06	1.34298E-09	7.02332E-07
0.65	1.56921E-06	4.66951E-06	1.30563E-06	1.27681E-06	7.53043E-08	8.68021E-07
0.7	1.51554E-06	5.42980E-06	1.40851E-06	1.23761E-06	9.53281E-08	8.49305E-07
0.75	1.31311E-06	5.90948E-06	1.37913E-06	8.22917E-07	3.31786E-08	6.87327E-07
0.8	1.09372E-06	6.05496E-06	1.39529E-06	4.67729E-07	1.63426E-08	6.48860E-07
0.85	1.32931E-06	5.86506E-06	1.46699E-06	8.17396E-07	6.71198E-09	9.54506E-07
0.9	1.68167E-06	5.93889E-06	1.69677E-06	9.63803E-07	3.03388E-07	9.65987E-07
0.95	1.74649E-06	6.86096E-06	1.77784E-06	1.03184E-06	1.67538E-07	9.49239E-07
1	1.28010E-06	4.67303E-06	1.33233E-06	9.98536E-07	5.68242E-08	6.78837E-07

Fig. 2 presents the optimal weights and result comparison for $I(\theta)$ and $R(\theta)$ of the MRS. The optimal weight vectors are illustrated plotted in Fig. 2(a-b) for the MRS, while the results are performed in Fig. 2(c-d) of the MRS. These overlapping of the mean, best and worst solutions is performed to check the correctness of the AI based MWNNs-PSOASP. Fig. 2(e) provides the AE performances for $I(\theta)$ and $R(\theta)$ of the MRS. For the $I(\theta)$ and $R(\theta)$ categories of the MRS,

the AE measures are performed around 10^{-06} to 10^{-08} and 10^{-07} to 10^{-08}. These calculated optimal performances based on the AE represent the exactness of the AI based MWNN-PSOASP.

Fig. 3 presents the statistical computing measures for the $I(\theta)$ and $R(\theta)$ classes of the MRS. The statistical TIC and MSE operators have been used to present the numerical solutions of the MRS. One can observe that the TIC values for $I(\theta)$ and $R(\theta)$ classes of the MRS are measured as 10^{-10}-10^{-11} and 10^{-11}-10^{-12}. The MSE operator values for both the classes $I(\theta)$ and $R(\theta)$ lie as 10^{-13}-10^{-14}. These performances indicate the correctness of the AI based MWNN-PSOASP for the MRS.

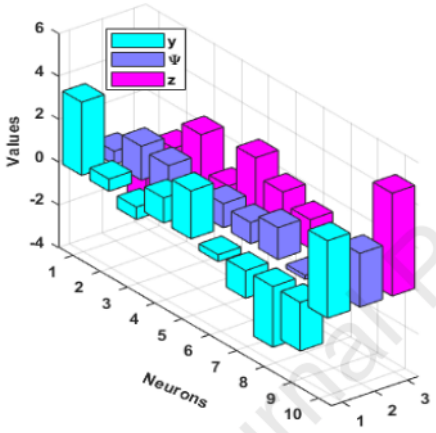

(a) Weights: $I(\theta)$

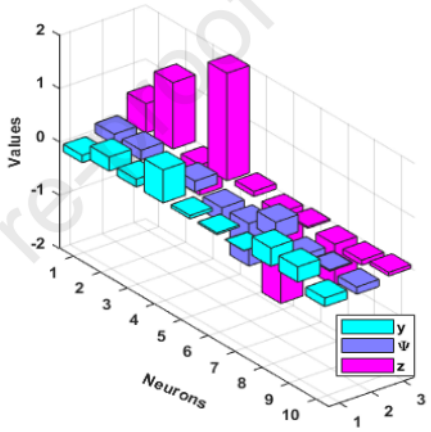

(b) Weights: $R(\theta)$

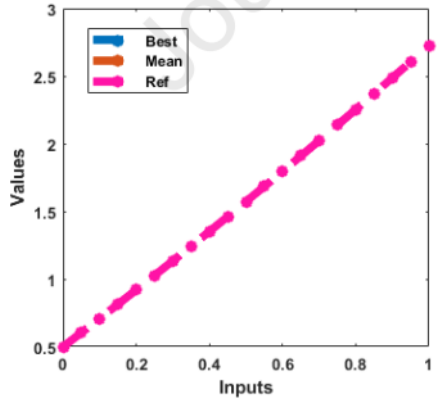

(c) Comparison: $I(\theta)$

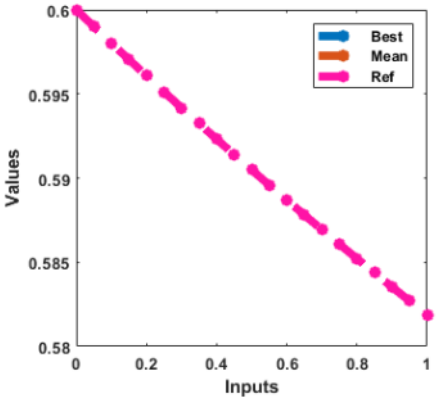

(d) Comparison: $R(\theta)$

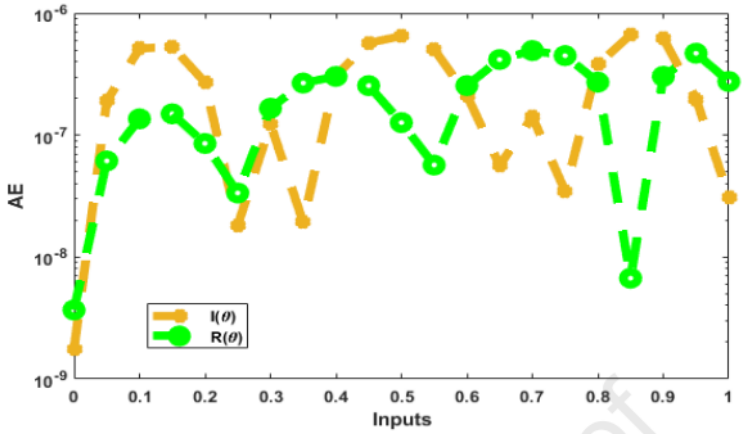

(e) AE values for $I(\theta)$ and $R(\theta)$

Figure 2: Optimal weights, comparison performances and AE for $I(\theta)$ and $R(\theta)$ of the MRS

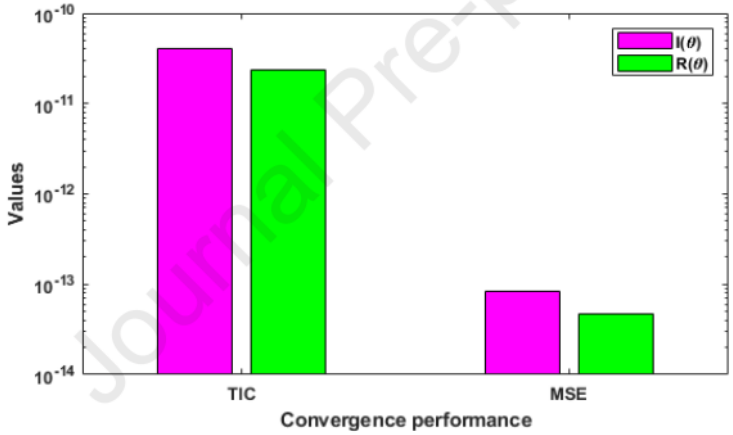

Figure 3: Performances of the statistical operators for $I(\theta)$ and $R(\theta)$ of the MRS

To check the consistency of the AI based MWNN-PSOASP for the MRS, the statistical TIC and MSE interpretations have been illustrated in Figs. 4-6. Twenty trials have been implemented in input domain [0,1] by taking 10 number of neurons. The TIC convergence values have been plotted as 10^{-09}-10^{-10} and 10^{-10}-10^{-11} for $I(\theta)$ and $R(\theta)$. Similarly, MSE convergence performances have been derived as 10^{-11}-10^{-13} and 10^{-12}-10^{-13} for $I(\theta)$ and $R(\theta)$ of the MRS. These optimal performances using the AI based MWNN-PSOASP authenticate that the proposed scheme performs well to solve the MRS.

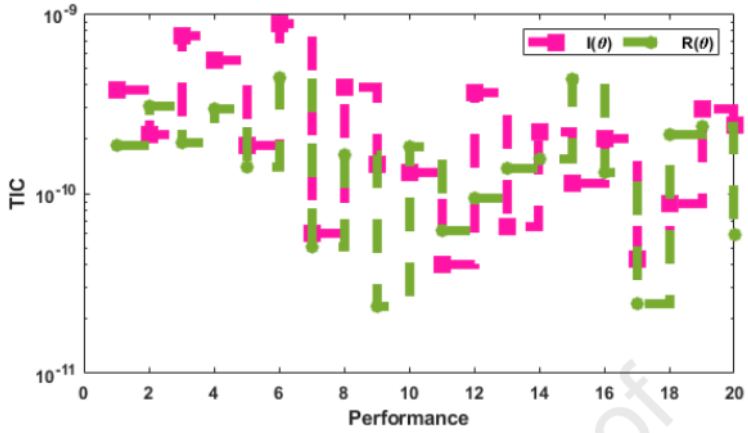

TIC operator measures for $I(\theta)$ and $R(\theta)$

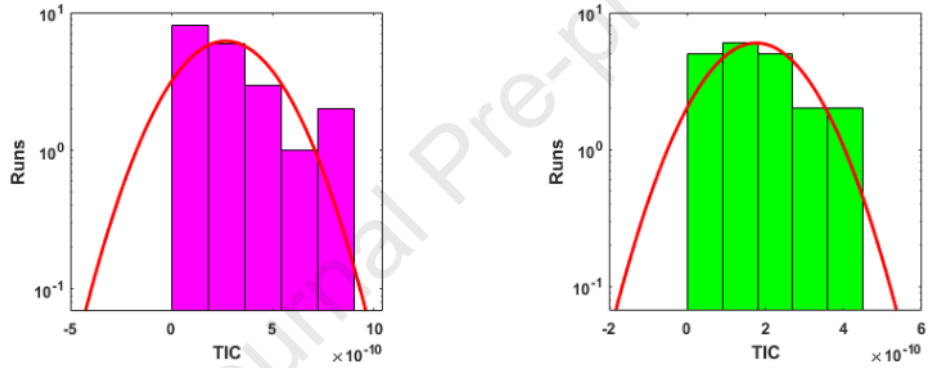

(a) HG: $I(\theta)$ **(b)** HG: $R(\theta)$

Figure 4: TIC operator convergence measures performances for $I(\theta)$ and $R(\theta)$ of the MRS

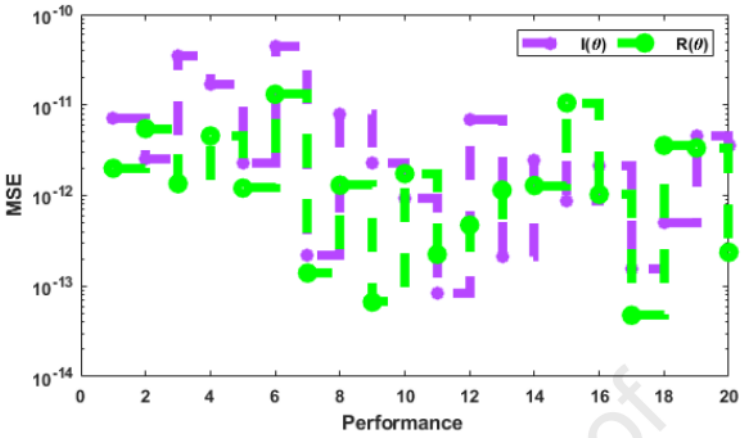

MSE operator measures for $I(\theta)$ and $R(\theta)$

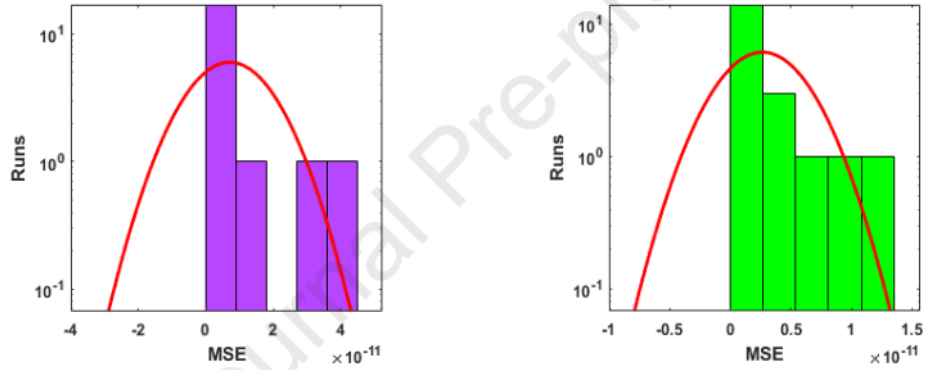

(a) HG: $I(\theta)$ **(b)** HG: $R(\theta)$

Figure 5: MSE operator convergence measures performances for $I(\theta)$ and $R(\theta)$ of the MRS

4. Concluding remarks

The purpose of these investigations is to present the numerical solutions of the mathematical robot system to examine the positive coronavirus cases. The design of the artificial intelligence-based Morlet wavelet neural network has been presented first time to solve the mathematical robot system. The mathematical robot system has been categorized into two dynamics, infected $I(\theta)$ and Robots $R(\theta)$. Few concluding remarks of this study are presented as:

- The design of the AI based MWNN along with the optimization efficiency of PSOASM is presented first time to solve the mathematical robot system.

- The proposed AI based MWNN-PSOAPS is effectively applied to solve the mathematical robot system.
- For the exactness of the AI based MWNN-PSOIPS, the comparison of the results has been presented by using the proposed and reference solutions.
- The reliability of the MWNN-PSOASP has been authenticated by extending the data into 20 trials to check the performance of the scheme through the statistical operators with 10 hidden numbers of neurons to solve the MRS.

Future research directions: The proposed AI based MWNN-PSOASP can be implemented to solve various nonlinear, fractional and fluid dynamic systems [49-55].

Declaration of competing interest

The authors declare that they have no known competing financial interests or personal relationships that could have appeared to influence the work reported in this paper.

Acknowledgement: The authors would like to thank the Deanship of Scientific Research at Umm Al-Qura University for supporting this work by Grant Code: (22UQU4282396DSR16).

References

[1] Side, S. and Noorani, M.S.M., 2013. A SIR model for spread of dengue fever disease (simulation for South Sulawesi, Indonesia and Selangor, Malaysia). World Journal of Modelling and Simulation, 9(2), pp.96-105.

[2] Bhatt, S., Gething, P.W., Brady, O.J., Messina, J.P., Farlow, A.W., Moyes, C.L., Drake, J.M., Brownstein, J.S., Hoen, A.G., Sankoh, O. and Myers, M.F., 2013. The global distribution and burden of dengue. Nature, 496(7446), pp.504-507.

[3] Guerrero–Sánchez, Y., Umar, M., Sabir, Z., Guirao, J.L. and Raja, M.A.Z., 2021. Solving a class of biological HIV infection model of latently infected cells using heuristic approach. Discrete & Continuous Dynamical Systems-S, 14(10), p.3611.

[4] Umar, M., Sabir, Z., Amin, F., Guirao, J.L. and Raja, M.A.Z., 2020. Stochastic numerical technique for solving HIV infection model of CD4+ T cells. The European Physical Journal Plus, 135(5), pp.1-19.

[5] Umar, M., Sabir, Z., Raja, M.A.Z., Aguilar, J.G., Amin, F. and Shoaib, M., 2021. Neuro-swarm intelligent computing paradigm for nonlinear HIV infection model with CD4+ T-cells. Mathematics and Computers in Simulation, 188, pp.241-253.

[6] McCormick, J.B., King, I.J., Webb, P.A., Johnson, K.M., O'Sullivan, R., Smith, E.S., Trippel, S. and Tong, T.C., 1987. A case-control study of the clinical diagnosis and course of Lassa fever. Journal of Infectious Diseases, 155(3), pp.445-455.

[7] Bushman, M., Antia, R., Udhayakumar, V. and de Roode, J.C., 2018. Within-host competition can delay evolution of drug resistance in malaria. PLoS biology, 16(8), p.e2005712.

[8] Smith, D.G. and Ferrell, R.E., 1980. A family study of the hemoglobin polymorphism in Macaca fascicularis. Journal of Human Evolution, 9(7), pp.557-563.

[9] Kakuru, A., Staedke, S.G., Dorsey, G., Rogerson, S. and Chandramohan, D., 2019. Impact of Plasmodium falciparum malaria and intermittent preventive treatment of malaria in pregnancy on the risk of malaria in infants: a systematic review. Malaria journal, 18(1), pp.1-13.

[10] Emond, R.T., Evans, B., Bowen, E.T. and Lloyd, G., 1977. A case of Ebola virus infection. Br Med J, 2(6086), pp.541-544.

[11] Umar, M., Sabir, Z., Raja, M.A.Z., Shoaib, M., Gupta, M. and Sánchez, Y.G., 2020. A stochastic intelligent computing with neuro-evolution heuristics for nonlinear SITR system of novel COVID-19 dynamics. Symmetry, 12(10), p.1628.

[12] Umar, M., Sabir, Z., Raja, M.A.Z., Amin, F., Saeed, T. and Guerrero-Sanchez, Y., 2021. Integrated neuro-swarm heuristic with interior-point for nonlinear SITR model for dynamics of novel COVID-19. Alexandria Engineering Journal, 60(3), pp.2811-2824.

[13] Sánchez, Y.G., Sabir, Z. and Guirao, J.L., 2020. Design of a nonlinear SITR fractal model based on the dynamics of a novel coronavirus (COVID-19). Fractals, 28(08), p.2040026.

[14] Redhwan, S.S., Abdo, M.S., Shah, K., Abdeljawad, T., Dawood, S., Abdo, H.A. and Shaikh, S.L., 2020. Mathematical modeling for the outbreak of the coronavirus (COVID-19) under fractional nonlocal operator. Results in Physics, 19, p.103610.

[15] Gao, W., Baskonus, H.M. and Shi, L., 2020. New investigation of bats-hosts-reservoir-people coronavirus model and application to 2019-nCoV system. Advances in Difference Equations, 2020(1), pp.1-11.

[16] Thabet, S.T., Abdo, M.S. and Shah, K., 2021. Theoretical and numerical analysis for transmission dynamics of COVID-19 mathematical model involving Caputo–Fabrizio derivative. Advances in Difference Equations, 2021(1), pp.1-17.

[17] Jeelani, M.B., Alnahdi, A.S., Abdo, M.S., Abdulwasaa, M.A., Shah, K. and Wahash, H.A., 2021. Mathematical Modeling and Forecasting of COVID-19 in Saudi Arabia under Fractal-Fractional Derivative in Caputo Sense with Power-Law. Axioms, 10(3), p.228.

[18] Ögren, P. and Martin, C.F., 2002. Vaccination strategies for epidemics in highly mobile populations. Applied Mathematics and Computation, 127(2-3), pp.261-276.

[19] Goufo, D., Franc, E., OukouomiNoutchie, S.C. and Mugisha, S., 2014. A fractional SEIR epidemic model for spatial and temporal spread of measles in metapopulations. In Abstract and Applied Analysis (Vol. 2014). Hindawi.

[20] Dietz, K., 1988. The first epidemic model: a historical note on PD En'ko. Australian Journal of Statistics, 30(1), pp.56-65.

[21] Hethcote, H.W., 2000. The mathematics of infectious diseases. SIAM review, 42(4), pp.599-653.

[22] Botmart, T., Sabir, Z., Raja, M.A.Z., Weera, W., Sadat, R. and Ali, M.R., 2022. A numerical study of the fractional order dynamical nonlinear susceptible infected and quarantine differential model using the stochastic numerical approach. Fractal and Fractional, 6(3), p.139.

[22] Wickwire, K., 1977. Mathematical models for the control of pests and infectious diseases: a survey. Theoretical population biology, 11(2), pp.182-238.

[23] Zhang, H., Jiao, J. and Chen, L., 2007. Pest management through continuous and impulsive control strategies. Biosystems, 90(2), pp.350-361.

[24] Baba, I.A., Baba, B.A. and Esmaili, P., 2020. A mathematical model to study the effectiveness of some of the strategies adopted in curtailing the spread of COVID-19. *Computational and mathematical methods in medicine*, *2020*.

[25] Sabir, Z., Raja, M.A.Z., Guirao, J.L. and Shoaib, M., 2020. Integrated intelligent computing with neuro-swarming solver for multi-singular fourth-order nonlinear Emden–Fowler equation. Computational and Applied Mathematics, 39(4), pp.1-18.

[26] Sabir, Z., Wahab, H.A., Javeed, S. and Baskonus, H.M., 2021. An efficient stochastic numerical computing framework for the nonlinear higher order singular models. Fractal and Fractional, 5(4), p.176.

[27] Sabir, Z., Khalique, C.M., Raja, M.A.Z. and Baleanu, D., 2021. Evolutionary computing for nonlinear singular boundary value problems using neural network, genetic algorithm and active-set algorithm. The European Physical Journal Plus, 136(2), pp.1-19.

[28] Sabir, Z., 2022. Stochastic numerical investigations for nonlinear three-species food chain system. International Journal of Biomathematics, 15(04), p.2250005.

[29] Souayeh, B., Sabir, Z., Umar, M. and Alam, M.W., 2022. Supervised Neural Network Procedures for the Novel Fractional Food Supply Model. Fractal and Fractional, 6(6), p.333.

[30] Sabir, Z., Ali, M.R. and Sadat, R., 2022. Gudermannian neural networks using the optimization procedures of genetic algorithm and active set approach for the three-species food chain nonlinear model. Journal of Ambient Intelligence and Humanized Computing, pp.1-10.

[31] Kiani, A.K., Khan, W.U., Raja, M.A.Z., He, Y., Sabir, Z. and Shoaib, M., 2021. Intelligent backpropagation networks with bayesian regularization for mathematical models of environmental economic systems. Sustainability, 13(17), p.9537.

[32] Y. Shi and R. C. Eberhart, "Empirical study of particle swarm optimization," In Proceedings of the 1999 Congress on Evolutionary Computation-CEC99, vol. 3, pp. 1945-1950, IEEE, 1999.

[33] A. P. Engelbrecht, "Computational intelligence: an introduction," 2nd ed., Chichester, U.K.: John Wiley & Sons Ltd., 2007.

[34] De Almeida, B.S.G. and Leite, V.C., 2019. Particle swarm optimization: A powerful technique for solving engineering problems. Swarm intelligence-recent advances, new perspectives and applications, pp.1-21.

[35] Zhang, X., Liu, H. and Tu, L., 2020. A modified particle swarm optimization for multimodal multi-objective optimization. Engineering Applications of Artificial Intelligence, 95, p.103905.

[36] Elsheikh, A.H. and Abd Elaziz, M., 2019. Review on applications of particle swarm optimization in solar energy systems. International Journal of Environmental Science and Technology, 16(2), pp.1159-1170.

[37] Yousri, D., Thanikanti, S.B., Allam, D., Ramachandaramurthy, V.K. and Eteiba, M.B., 2020. Fractional chaotic ensemble particle swarm optimizer for identifying the single, double, and three diode photovoltaic models' parameters. Energy, 195, p.116979.

[38] Darwish, A., Ezzat, D. and Hassanien, A.E., 2020. An optimized model based on convolutional neural networks and orthogonal learning particle swarm optimization algorithm for plant diseases diagnosis. Swarm and evolutionary computation, 52, p.100616.

[39] Junior, F.E.F. and Yen, G.G., 2019. Particle swarm optimization of deep neural networks architectures for image classification. Swarm and Evolutionary Computation, 49, pp.62-74.

[40] Chen, H., Fan, D.L., Fang, L., Huang, W., Huang, J., Cao, C., Yang, L., He, Y. and Zeng, L., 2020. Particle swarm optimization algorithm with mutation operator for particle filter noise reduction in mechanical fault diagnosis. International journal of pattern recognition and artificial intelligence, 34(10), p.2058012.

[41] Cui, Z., Zhang, J., Wu, D., Cai, X., Wang, H., Zhang, W. and Chen, J., 2020. Hybrid many-objective particle swarm optimization algorithm for green coal production problem. Information Sciences, 518, pp.256-271.

[42] Gurriet, T., Singletary, A., Reher, J., Ciarletta, L., Feron, E. and Ames, A., 2018, April. Towards a framework for realizable safety critical control through active set invariance. In 2018 ACM/IEEE 9th International Conference on Cyber-Physical Systems (ICCPS) (pp. 98-106). IEEE.

[43] Zhang, C. and Chen, X., 2020. A smoothing active set method for linearly constrained non-lipschitz nonconvex optimization. SIAM Journal on Optimization, 30(1), pp.1-30.

[44] Kasinathan, G., Jayakumar, S., Gandomi, A.H., Ramachandran, M., Fong, S.J. and Patan, R., 2019. Automated 3-D lung tumor detection and classification by an active contour model and CNN classifier. Expert Systems with Applications, 134, pp.112-119.

[45] Shi, H., Wang, H., Qin, C., Zhao, L. and Liu, C., 2020. An incremental learning system for atrial fibrillation detection based on transfer learning and active learning. Computer methods and programs in biomedicine, 187, p.105219.

[46] Wang, Y., Olaru, S., Valmorbida, G., Puig, V. and Cembrano, G., 2019. Set-invariance characterizations of discrete-time descriptor systems with application to active mode detection. Automatica, 107, pp.255-263.

[47] Piller, O., Elhay, S., Deuerlein, J. and Simpson, A., 2020. A content-based active-set method for pressure-dependent models of water distribution systems with flow controls. Journal of Water Resources Planning and Management, 146(4), pp.04020009-13.

[48] Klaučo, M., Kalúz, M. and Kvasnica, M., 2019. Machine learning-based warm starting of active set methods in embedded model predictive control. Engineering Applications of Artificial Intelligence, 77, pp.1-8.

[49] Durur, H. and Yokuş, A., 2021. Exact solutions of (2+ 1)-Ablowitz-Kaup-Newell-Segur equation. Applied Mathematics and Nonlinear Sciences, 6(2), pp.381-386.

[50] Sulaiman, T.A., Bulut, H. and Baskonus, H.M., 2021. On the exact solutions to some system of complex nonlinear models. Applied Mathematics and Nonlinear Sciences, 6(1), pp.29-42.

[51] 8. Sajjan, N.A. Shah, N.A. Ahammad, C.S.K. Raju, M.D. Kumar, W. Weera, Nonlinear Boussinesq and Rosseland approximations on 3D flow in an interruption of Ternary nanoparticles with various shapes of densities and conductivity properties, AIMS Mathematics, 7(10), (2022), 18416-18449.

[52] P. Priyadharshini, M. V. Archana, N. A. Ahmmad, C.S.K Raju, S-J Yook, N.A. Shah, Gradient descent machine learning regression for MHD flow: Metallurgy process, International Communications in Heat and Mass Transfer, 138 (2022), 106307.

[53] Erdogan, F., Sakar, M.G. and Saldır, O., 2020. A finite difference method on layer-adapted mesh for singularly perturbed delay differential equations. Applied Mathematics and Nonlinear Sciences, 5(1), pp.425-436.

[54] Sabir, Z., Sakar, M.G., Yeskindirova, M. and Saldir, O., 2020. Numerical investigations to design a novel model based on the fifth order system of Emden–Fowler equations. Theoretical and Applied Mechanics Letters, 10(5), pp.333-342.

[55] Ayub, A., Wahab, H.A., Sabir, Z. and Arbi, A., 2020. A note on heat transport with aspect of magnetic dipole and higher order chemical process for steady micropolar fluid. Computational Overview of Fluid Structure Interaction, 97.

Acknowledgements

Authors would like to thank Prof. Jianguo Gao for his guidance during the writing of the paper, and sincerely thank the editors for their careful evaluation of the paper.

Declaration of competing interest

The authors declare that they have no known competing financial interests or personal relationships that could have appeared to influence the work reported in this paper.

Swarming morlet wavelet

ORIGINALITY REPORT

9%	7%	8%	3%
SIMILARITY INDEX	INTERNET SOURCES	PUBLICATIONS	STUDENT PAPERS

PRIMARY SOURCES

1	Submitted to St George's Hospital Medical School Student Paper	1%
2	Submitted to National University of Ireland, Galway Student Paper	1%
3	Botmart, Thongchai, Narongsak Yotha, Kanit Mukdasai, and Supreecha Wongaree. "GLOBAL SYNCHRONIZATION FOR HYBRID COUPLED NEURAL NETWORKS WITH INTERVAL TIME-VARYING DELAYS : A MATRIX-BASED QUADRATIC CONVEX APPROACH", Asian-European Journal of Mathematics, 2016. Publication	1%
4	fusionsites.ciemat.es Internet Source	1%
5	Yiming Liu, Shuang Jian, Jianguo Gao. "Dynamics analysis and optimal control of SIVR epidemic model with incomplete immunity", Advances in Continuous and Discrete Models, 2022	1%

Publication

6	www.nature.com Internet Source	1 %
7	Prem Junsawang, Samina Zuhra, Zulqurnain Sabir, Muhammad Asif Zahoor Raja, Muhammad Shoaib, Thongchai Botmart, Wajaree Weera. "Numerical Simulations of Vaccination and Wolbachia on Dengue Transmission Dynamics in the Nonlinear Model", IEEE Access, 2022 Publication	<1 %
8	Gaurav Gupta, Puneet Rana. "Comparative Study on Rosseland's Heat Flux on Three-Dimensional MHD Stagnation-Point Multiple Slip Flow of Ternary Hybrid Nanofluid over a Stretchable Rotating Disk", Mathematics, 2022 Publication	<1 %
9	Nabeela Anwar, Muhammad Shoaib, Iftikhar Ahmad, Shafaq Naz, Adiqa Kausar Kiani, Muhammad Asif Zahoor Raja. "Intelligent computing networks for nonlinear influenza-A epidemic model", International Journal of Biomathematics, 2022 Publication	<1 %
10	scirp.org Internet Source	<1 %
11	www.sciendo.com Internet Source	

		<1 %
12	Zulqurnain Sabir, Hafiz Abdul Wahab, Tri Gia Nguyen, Gilder Cieza Altamirano, Fevzi Erdoğan, Mohamed R. Ali. "Intelligent computing technique for solving singular multi-pantograph delay differential equation", Soft Computing, 2022 Publication	<1 %
13	Zulqurnain Sabir, Muhammad Asif Zahoor Raja, Muhammad Umar, Muhammad Shoaib. "Neuro-swarm intelligent computing to solve the second-order singular functional differential model", The European Physical Journal Plus, 2020 Publication	<1 %
14	ebin.pub Internet Source	<1 %
15	www.naturalspublishing.com Internet Source	<1 %
16	Zulqurnain Sabir, Muhammad Umar, Muhammad Asif Zahoor Raja, Haci Mehmet Baskonus, Wei Gao. "Designing of Morlet wavelet as a neural network for a novel prevention category in the HIV system", International Journal of Biomathematics, 2021 Publication	<1 %

17	bmcpublichealth.biomedcentral.com Internet Source	<1%
18	www.intechopen.com Internet Source	<1%

Exclude quotes	On	Exclude matches	< 10 words
Exclude bibliography	On		